Journal of Engineering Science and Technology
Vol. 6, No. 4 (2011) 481 - 492

BEST FIT MODELS TEST FOR THE VIRTUAL CHANNEL IN DISTRIBUTED VIDEO CODING

A. ELAMIN*, VARUN JEOTI, SAMIR BELHOUARI

Electrical Eng., Unievrsiti Teknologi PETRONAS, Perak, Malaysia
*Corresponding Author: eaea33@itu.dk

Abstract

Wyner-Ziv (WZ) video coding – a particular case of distributed video coding (DVC) – is a new video coding paradigm based on two major Information Theory results: the Slepian-Wolf and Wyner-Ziv theorems. Most of the solutions available in the literature, model the correlation noise between the original frame and the so-called side information by virtual channel. However most of the DVC solutions in the literature assume Laplacian distribution as noise virtual channel model, in this study we perform three goodness-of-fit tests, the Kolmogorov-Smirnov test and the Chi-Square test and log-Likelihood test to study the nature of the virtual channel. The results show that a mixture of 3 (or 4) mixture Gaussian model can best describe this virtual channel.

Keywords: Distributed video coding, Virtual channel model, KS test,
Chi-square test, Log-likelihood ratio test.

1. Introduction

Conventional digital video coding paradigm represented by the ITU-T and MPEG standards mainly relies on a hybrid of block-based transform and inter-frame predictive coding approaches. In this coding framework, the encoder exploits both the temporal and spatial redundancies present in the video sequence, which is a complex process and it requires a noticeable amount of resources (power and memory). As a result, all standard video encoders have much higher computational complexity than the decoder (typically five to ten times more complex) [1], mainly due to the temporal correlation exploitation tools used in the motion estimation task. As a result, the traditional video coding is no longer applicable for these WVSN applications. Appropriate video coding paradigm for these applications must have low encoding complexity.

Lower encoding complexity can be achieved by moving some of the encoder tasks to the decoder part, particularly the complex motion estimation process. Two notable theorems from information theory have paved the way for new video coding paradigm known in the literature as Distributed Video Coding (DVC). It allows low encoding complexity and approaches the efficiency of traditional video coding schemes. These two theorems are known as Slepian-Wolf theorem and Wyner-Ziv theorem [2, 3]. They suggest that, for two correlated sources X and Y, separate encoding - joint decoding system can approach the efficiency of joint encoding-decoding system when the information about the correlation between X and Y is available at the decoder. The practical application of DVC [4-9] is referred to as Wyner-Ziv video coding (WZ) where an estimate of the original frame herein called the "side information" is available at the decoder. The compression is achieved by sending only that extra information (parity bits) that is needed to correct this estimate. An error correcting code is often used with the assumption that the estimate is a noisy version of the original frame and the correction can be made with few extra parity bits that determine the rate.

For the purpose of modelling, a virtual channel is assumed to represent the estimation noise [10] in the estimate of the original frame. Many works [10-19] have been devoted to study this estimation noise and gain some insight of the characteristics of the virtual channel.

In this work the authors performed different goodness-of-fit test to identify the best fit model that characterizes the virtual channel. In this paper we will first introduce the theoretical foundation for the distributed source coding in Section 2. The modelling of the virtual channel is discussed in Section 3. The distribution models that have a potential in modelling the virtual channel are explained in Section 4. The goodness-of-fit tests will be covered in more detail in Section 5. The experimental work and its results will be explained in Section 6. Section 7 concludes the work and presents the future work.

2. Theoretical Foundation

Let $\{(X_i,Y_i)\}$ be a sequence of independent and identically distributed (i.i.d.) drawings of a pair of correlated discrete random variables X and Y. For lossless compression with arbitrarily small error $X = \hat{X}$ and $Y = \hat{Y}$ after decompression, it is known from Shannon's source coding theorem that a rate given by the joint entropy, $H(X,Y)$, of X and Y is sufficient if the two sources are jointly encoded . For example, we can first compress Y into $H(Y)$ bits per sample, and based on the complete knowledge of Y at the encoder and the decoder, then compress X into $H(X,Y)$ bits per sample. But if X and Y must be separately encoded for some user to reconstruct both of them the sufficient rate for lossless reconstruction is not known. One can separately encode them with rate, $R=H(X)+H(Y)$, which is greater than $H(X,Y)$ if the two sources X and Y are correlated. In 1973, Slepian and Wolf [2] showed that $R=H(X,Y)$is sufficient for lossless decompression, even for separate encoding of correlated sources (see Fig. 1).

In other words, for the rates

$$\begin{aligned} R_X &\geq H(X,Y) \\ R_Y &\geq H(X,Y) \end{aligned} \tag{1}$$

The combined rate is given by

$$R_X + R_Y \geq H(X,Y) \tag{2}$$

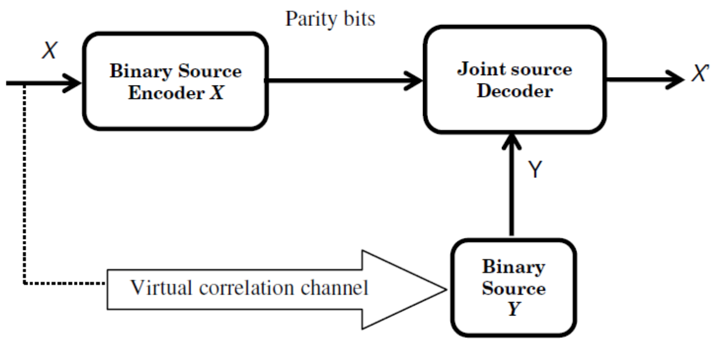

Fig. 1. Relationship between Channel Coding and Slepian-Wolf Coding.

The proof of the Slepian-Wolf theorem is based on random binning, which is non-constructive, i.e., it does not reveal how practical code design should be done [20]. Wyner suggested the use of channel coding to approach the R=H(X)+H(Y) SW rate. Consider a binary sequence, X, to be encoded and a noisy version of it, Y, present at the decoder (Fig. 1). To correct the errors between these two binary sequences, a channel code may be applied to the sequence X. The compression of X is achieved by transmitting only the parity bits. Hence, jointly with Y, the decoder uses the parity bits produced by the encoder to make error correction, achieving a perfect decoding of the sequence X.

Wyner and Ziv [3] have studied a particular case of Slepian-Wolf coding corresponding to the rate point (H(Y), H(X|Y)) where X and Y are correlated sources. The work of Wyner-Ziv [3] has established the rate-distortion (RD), $R^*_{X|Y}(D)$, necessary to encode X guaranteeing its reconstruction with an average distortion below D, assuming that only the decoder has access to Y. The results obtained by Wyner and Ziv indicate that when the statistical dependency between X and Y is exploited only at the decoder, the transmission rate increases compared to the case where the correlation is exploited both at the encoder and the decoder, for the same average distortion, D. Mathematically, the Wyner and Ziv theorem can be described by

$$R^*_{X|Y}(D) \geq R_{X|Y} \qquad\qquad D \geq 0 \tag{3}$$

where $R^*_{X|Y}(D)$ represents the minimum encoding rate for X and H(X|Y) represents the minimum rate necessary to encode X when Y is available at the encoder and the decoder. Wyner and Ziv showed that there is no rate increase for all $D \geq 0$, when X and Y are jointly Gaussian sequences and D, an MSE distortion measure. A major work on practical Wyner-Ziv code design called DISCUS [21] recently extended the no rate loss condition for Wyner-Ziv coding even for case where only the innovation between X and Y is Gaussian, and X and Y could follow more general distributions.

3. Modelling the Virtual Channel

Distributed source coders rely heavily on efficient error correcting codes, the performance of these codes depends greatly on the choice of the noise model that characterizes the dependency channel [6]. The no loss result of the Slepian-Wolf theorem comes under the assumption that the statistical dependence between WZ data and SI is perfectly known to both encoder and decoder, and that it follows a Gaussian distribution [2]. Exact knowledge of the statistical dependence between X and Y is required

- to characterize the channel in the SW decoder,
- to perform MMSE estimation in the inverse quantizer, and
- to help controlling the SW code rate [22, 23].

It is widely common in DVC literature [6-12] to use a Laplacian distribution to model the statistical correlation between the original frame and the side information, this Laplacian distribution is used to convert the side information (pixel values) into soft-input information needed for channel decoding. In first DVC implementations, the Laplacian parameters were off-line computed for each sequence [4].

The correlation between the decoder SI and the original WZ frame is estimated at the encoder by recreating the SI for each WZ frame as the average of the two temporally closer key frames [17]. Furthermore, the bit error probability of each bit plane is modelled assuming a Binary Symmetric Channel (BSC). In the SEASON framework [24], the deviation of the side information from the actual video frame is modelled as an additive stationary white noise signal. With the use of Turbo codes as Slepian-Wolf coder, an inaccurately chosen noise model of the dependency channel (modelled by the conditional *pdf* $P(X|Y)$ has a big influence on the performance of Turbo decoding [13]. The performance loss due to the inaccuracies in modelling the non-stationary dependency channel and the sensitivity of LDPC codes to the modelling of the noise in the dependency channel is experimentally has been studied in [25].

The pixel domain DVC is simplest DVC system where the spatial correlation is ignored and only the temporal correlation is utilized to obtain good compression ratio. In this system the virtual represents the correlation between the quantized original pixel values and the side information pixel values. The transform domain distributed video codec exploits the spatial redundancy within a frame, by applying the DCT transform over the frame blocks; therefore the DCT transform coefficients are grouped into DCT bands and then quantized and turbo coded, since DCT coefficient are turbo coded the noise must be taken to represent the correlation noise between the original frame quantized DCT bands and the side information DCT bands.

4. Probability Distributions

A commonly used distribution distributions will be considered here in this study such as the Gaussian, Laplacian and Gaussian Mixture models. The Gaussian and Laplacian distribution have been used to model the virtual channel in many DVC solutions, both models represent stationary noise. The Gaussian mixture also is considered to investigate the non-stationary model for the virtual channel. The Gaussian *pdf* with mean μ and variance σ^2 is defined by

$$f_X(x) = \frac{1}{\sqrt{2\pi\sigma}} e^{-\frac{(x-\mu)^2}{2\sigma^2}} \tag{4}$$

The Laplacian *pdf* with parameters μ and $\frac{2}{\gamma^2}$

$$f(x) = \frac{\gamma}{2} e^{-\gamma|x-\mu|} \tag{5}$$

The Gaussian mixture *pdf* with the parameters σ^2, ρ_i, μ_i model can be defined by

$$f(x) = \sum_{i=1}^{K} \frac{\rho_i}{\sqrt{2\pi\sigma}} e^{-\frac{(x-\mu)^2}{2\sigma^2}} \tag{6}$$

Goodness-of-fit test

Goodness-of-fit tests are used to examine hypothesis that a given data set comes from a model distribution with given parameters. The Kolmogorov-Smirnov [26] (KS) test and Chi-Square tests are two popular goodness-of-fit tests. The KS test has been used in [16, 18-20, 22], to study the statistics of DCT coefficients, chi-square has also been used to characterize the distribution of the DCT [5-7].

5.1. Kolmogorov-Smirnov goodness-of-fit test

Kolmogorov–Smirnov test compares the empirical cumulative distribution function (ECDF) with the given model CDF. Given N ordered data points $X_1, X_2, \ldots, X_N$, the ECDF is defined as

$$\hat{F}_X(x) = \begin{cases} 0 & x < x_1 \\ \frac{n}{M} & x_n < x < x_{n+1} \quad n = 1, 2, \cdots M \\ 1 & x < x_M \end{cases} \tag{7}$$

The KS statistic D_n is then defined as

$$D_n = \max_{i=1,2,\cdots M} \left| F_X(x_i) - \hat{F}_X(x_i) \right| \tag{8}$$

The KS statistic test measure the distance between the empirical CDF and the model CDF which would measure the goodness-of-fit. If the empirical CDF is tested against several model CDFs, the model that gives the minimum KS statistic can be taken to be the best fit for the data.

5.2. The chi-square goodness-of-fit test

The Chi-square compares probability density functions (*pdf*).This test is applied to binned data (i.e., data is divided into disjoint classes, for non-binned data chi-square test can simply be performed on the histogram or frequency table of the non-binned data. This test is sensitive to the choice of bins. There is no optimal choice for the bin width (since the optimal bin width depends on the distribution). Assume we have k A-bins A_i; i = 1, 2, …., k. Let $E_i = np_i$ the expected frequency in bin A_i with $p_i = P(x \in A_i)$ and n the total number of data samples. Let O_i be the observed frequency in bin A_i then the Chi-square statistic is defined as

$$V_k = \sum_{i=1}^{k} \frac{O_i - E_i}{E_i} \tag{9}$$

The V_i is the measure of deviation of the empirical frequencies from the expected frequencies. Best fit model is the one that gives the minimum chi-square statistic.

5.3. The log-likelihood ratio goodness-of-fit test

The Likelihood Ratio Test (LRT) is a statistical test of the goodness-of-fit between two models $F_x(x)$ and $G_x(x)$. A relatively more complex model is compared to a simpler model to see if it fits a particular dataset significantly better. If so, the additional parameters of the more complex model are often used in subsequent analyses. The LRT is only valid if used to compare hierarchically nested models. That is, the more complex model must differ from the simple model only by the addition of one or more parameters. Adding additional parameters will always result in a higher likelihood score. The LRT provides one objective criterion for selecting among possible models. The LRT begins with a comparison of the likelihood scores of the two models:

$$LLR = \log\left\{\frac{F_x(x_1)\times F_x(x_2)\times\cdots\cdots F_x(x_n)}{G_x(x_1)\times G_x(x_2)\times\cdots\cdots G_x(x_n)}\right\} \tag{10}$$

This LRT statistic approximately follows a chi-square distribution.

5. Experiments and Results

Table 1 gives the detail of the video sequences set used in this study. This set of sequences represents a range of typical video content from low and high latency applications. This set has been used in many related studies and video coding performance testing. The frame interpolation is performed by motion compensation as in [1], for GOP = 2. The quantization scheme for the transform domain as in [1] and only tow RD point were considered. Each chosen sequence provides 25344×100 samples for pixel domain and 1584×100 samples per coefficient for transform domain. Therefore, the empirical distribution derived from these sequences can be assumed to be close to the actual distributions.

The virtual channel in the transform domain is to model the correlation between the original frame bands and estimate frame bands. The typical bands number is 16 bands resulting from transforming 4-by-4 block into DCT transform. The test was performed on the first 15 bands and the 16th band is ignored due to its small energy. The number of the mixtures model used to model each DCT band is given in Table 2. The test results for the transform domain and for the pixel domain for different test sequences are given in Tables 3 to 8.

Table 1. Test Video Sequences.

	Sequence	Resolution QCIF	Number of Frames
1	Akiyo	176 × 144	296
2	Foreman	176 × 144	160
3	Container	176 × 144	296
4	News	176 × 144	296
5	Silent	176 × 144	296
6	Mother-daughter	176 × 144	296
7	Salesman	176 × 144	144
8	Paris	176 × 144	248
9	Miss America	176 × 144	160

Table 2. GMM Number per DCT Band.

3	3	3	2
3	3	2	2
3	3	2	2
2	2	2	0

The KS statistics were computed for the correlation under consideration against the distribution models. The distribution that gives the minimum KS statistics is chosen as the one that best fit under the KS criterion. Similarly for the Chi square the distribution that gives the minimum Chi-square statistics is chosen as the one that best fit under the Chi-square criterion. The log-likelihood ratio test is performed to compare different models to examine the goodness-fit to represent the virtual channel. The positive sign indicates the model in the numerator fits better than the de-numerator model.

The KS test results for transform domain and pixel domain are given in Tables 3 and 6 respectively. The Chi-square test results for the transform domain are given in Table 4 and for pixel domain for different test sequences are given in Table 7. Tables 5 and 8 show the test results for the log-likelihood ratio test for transform domain and pixel domain respectively.

The minimum statistics and the best fit distribution have been indicated in bold. The difference in the choice of best fit model for the virtual channel, based on the goodness statistics are only statistical and the performance of using this models has not been investigated in terms of RD performance of DVC systems. Although for some tests as in Table 3, the KS statistics show that the normal distribution fits better than Gaussian mixture but form all the tables the virtual channel can be seen as Gaussian mixture model in both domains (pixel and transform). The Chi-square tests' results also show that Gaussian mixture models fit better and the second best model is the Laplacian model. The consolidating test performed by log-likelihood test, also shows that the Gaussian mixture model is the best fit. The LLR test's result shows that the Laplacian distribution and normal distribution almost have equal statistics to represent the virtual channel.

Table 3. KS Test Results in the Transform Domain.

	Akiyo KS statistics			Foreman KS statistics		
Coef.	**Lap**	**GMM**	**Normal**	**Lap**	**GMM**	**Normal**
1	0.7326	**0.0728**	0.1460	0.4701	**0.0476**	0.1758
2	0.7735	**0.1060**	0.1346	0.5863	**0.0517**	0.1221
3	0.7419	**0.0982**	0.1588	0.5099	**0.0545**	0.1395
4	0.8178	**0.1256**	0.1281	0.6113	**0.0766**	0.1021
5	0.8203	**0.1364**	0.1547	0.5649	**0.0706**	0.1129
6	0.8584	**0.1029**	0.1128	0.7345	**0.0811**	0.1035
7	0.8942	**0.1513**	0.1742	0.8194	**0.1278**	0.1290
8	0.9153	0.1277	**0.1243**	0.6953	**0.0853**	0.0978
9	0.9051	0.1425	**0.1359**	0.6988	0.1723	**0.0917**
10	0.9063	**0.1670**	0.1739	0.7608	0.1675	**0.1003**
11	0.9667	0.1946	**0.1920**	0.8216	**0.1081**	0.1148
12	0.9418	0.1400	**0.1183**	0.8409	**0.0788**	0.0917
13	0.9521	0.2001	**0.1558**	0.8065	0.1693	**0.1274**
14	0.9850	0.1369	0.1175	0.9516	0.1894	**0.1303**
15	0.9832	**0.1485**	0.1699	0.9294	0.1581	**0.1149**

Table 4. Chi-Square Test Results in the Transform Domain.

	Akiyo Chi-Square statistics			Foreman Chi-Square statistics		
Coef.	**GMM**	**Lap**	**Normal**	**GMM**	**Lap**	**Normal**
1	**0.051 K**	1.352 K	1259.56 K	**0.053 K**	1.506 K	1259.44 K
2	**0.052 K**	1.349 K	1278.56 K	**0.078 K**	1.968 K	1606.64 K
3	**0.051 K**	1.166 K	1255.00 K	**0.045 K**	0.609 K	1242.11 K
4	**0.077 K**	1.397 K	1296.56 K	**0.067 K**	0.891 K	1203.80 K
5	**0.056 K**	1.347 K	1360.29 K	**0.051 K**	0.064 K	1379.46 K
6	**0.065 K**	0.833 K	1474.80 K	**0.050 K**	1.451 K	1620.30 K
7	**0.045 K**	4.053 K	1556.14 K	**0.026 K**	0.359 K	2368.20 K
8	**0.068 K**	16.542 K	1278.52 K	**0.016 K**	2.228 K	2798.99 K
9	**0.066 K**	8.1065 K	1398.93 K	**0.053 K**	8.605 K	1297.12 K
10	**0.109 K**	2.496 K	1267.39 K	**0.020 K**	0.370 K	1158.41 K
11	**0.080 K**	3.346 K	1347.63 K	**0.107 K**	0.059 K	1761.11 K
12	**0.113 K**	2.912 K	1295.42 K	**0.010 K**	49.58 K	1417.26 K
13	**0.079 K**	5.994 K	1268.11 K	**0.371 K**	2.998 K	6298.83 K
14	**0.057 K**	18.555 K	1255.70 K	**0.121 K**	10.46 K	2353.14 K
15	**0.070 K**	0.553 K	1300.64 K	**0.041 K**	0.062 K	1090.93 K

Table 5. Log-likelihood Ratio Test Results in the Transform Domain.

	Mother & Daughter LLR test result			Hall Transform domain LLR test result		
Coef.	**GMM/ Lap**	**Gauss/ GMM**	**Lap/ Normal**	**GMM/ Lap**	**Gauss/ GMM**	**Lap/ Normal**
1	7.2123	-7.2110	-0.0013	0.7037	-0.7037	-0.0000
2	2.3672	-2.3309	-0.0362	0.2163	-0.2125	-0.0038
3	2.3587	-2.3257	-0.0330	0.2309	-0.2267	-0.0041
4	3.4923	-3.4649	-0.0274	0.3149	-0.3112	-0.0037
5	3.8031	-3.7707	-0.0324	0.3693	-0.3658	-0.0036
6	4.0932	-4.0932	-0.0000	0.2738	-0.2709	-0.0030
7	7.3676	-7.3395	-0.0281	0.3886	-0.3854	-0.0032
8	5.4445	-5.4194	-0.0251	0.5384	-0.5356	-0.0029
9	5.3688	-5.3464	-0.0224	0.4914	-0.4884	-0.0030
10	6.2237	-6.1906	-0.0332	0.4601	-0.4568	-0.0033
11	9.9520	-9.9344	-0.0176	0.7218	-0.7197	-0.0021
12	8.2311	-8.2127	-0.0184	0.7969	-0.7969	-0.0000
13	9.7391	-9.7391	-0.0000	0.8768	-0.8768	-0.0000
14	∞	$-\infty$	-0.0000	1.0086	-1.0086	-0.0000
15	∞	$-\infty$	-0.0000	0.9369	-0.9369	-0.0000

Table 6. KS in Pixel Domain Test Results.

Test sequence	Lap	GMM	Normal
Carphone	0.7570	**0.0485**	0.0843
Miss-America	0.7007	**0.0456**	0.1108
Foreman	0.7121	**0.0780**	0.0869
Hall monitor	0.7543	**0.0397**	0.0530
Coastguard	0.6749	**0.0390**	0.1079
Akyio	0.7801	**0.0628**	0.0640
Mother & Daughter	0.7854	**0.0683**	0.1014

Table 7. Chi-Square Test Results for the Pixel Domain.

Video sequence	GMM	Laplace	Normal
Carphone	**0.8260K**	430.0K	323635. K
Miss-America	**0.7760K**	1094.4K	321467. K
Foreman	**0.8329K**	815.7K	321412. K
Hall	**0.8246K**	169.4K	321610. K
Coastgaurd	**0.8165K**	664.9K	321171. K
Akiyo	**1.1673k**	817.9K	322543. K
Mother daughter	**0.7425k**	425.3K	321801. K
News	**0.8615K**	812.2K	321407. K
Hall	**0.8246K**	169.4K	321610. K

Table 8. Log-likelihood Ratio Test Result for Pixel Domain.

Video Sequence	GMM/ Laplce	Normal/ GMM	Normal/ Laplace
Foreman	5.5226	-5.3646	-0.1580
Akyio	3.9404	-3.988	0.0476
Mother & daughter	2.1692	-2.1977	0.0284
Hall	2.9008	-2.9518	0.0510
News	7.2305	-6.6602	-0.5704
Salesman	4.531	-4.4336	-0.0974

Figures 2 and 3 show the histogram of the virtual channel and the empirical pdf of the actual data compared with the Gaussian and Laplacian distributions. From these figures we can see that the empirical pdf of the actual data can poorly be modelled by any of the two distributions, which validates the results shown in the tables that best model for the virtual channel is mixture of stationary models.

It is not surprising that the mixture model fits better than the stationary models (Gaussian and Laplacian) since the predicted frame is expected to have varying degrees of success along the predicted frame, although more sophisticated motion estimation/compensation algorithms can be used to generate the side information. The practical frame prediction is fundamentally faulty due to events like occlusions. In regions where the motion estimation process is successful like the background region the side information is much correlated with the original frame, in some other regions this process completely fails, caused by occlusion, the side information is uncorrelated with the original data. The limitations of side information prediction result in location-specific non-stationary estimation noise, for example, when occlusion occurs. As a result of the spatial variation in the side information, the noise process for the entire frame is represented by a group of uniform *pdf* models.

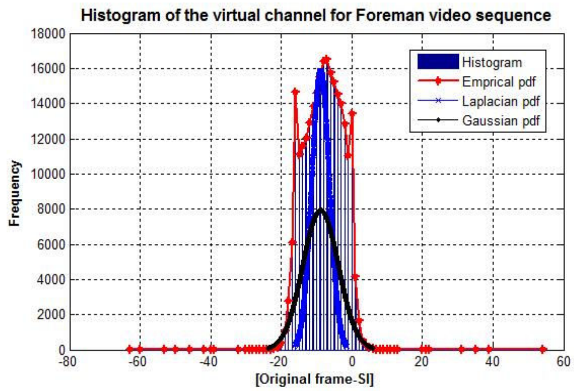

Fig. 2. Histogram of the Virtual Channel in Pixel Domain for Foreman Video Sequence.

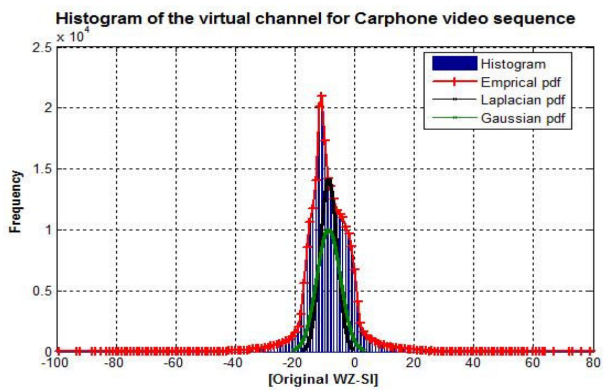

Fig. 3. Histogram of the Virtual in Transform Domain for Carphone Video Sequence.

6. Conclusions and Future Work

This study performs three goodness-of-fit tests to study the nature of the virtual channel in the feedback channel approach. However study shows that the best fit model is Gaussian mixture, which is non-stationary form. The non-stationary nature of the virtual channel is attributed to the fact that the side information estimations' quality varies along the frame, successful estimation at some regions and poor estimation at occluded regions. Therefore a better RD performance is expected to be obtained in systems that assume non-stationary model for the Virtual channel .This knowledge can enable design of optimal quantizer as well to improve the RD performance. If the virtual channel is assumed to be stationary extra attention must be given to the side information generation. Future work is implementing the DVC coding system to study the R-D performance of these models at the same setting to compare their capability to model the virtual channel and the impact of the accurate virtual channel modelling on R-D performance.

References

1. Aaron, A.; Rane, S.; Setton, E.; and Girod, B. (2004). Transform-domain Wyner-Ziv codec for video. *Proceedings of SPIE Visual Communications and Image Processing*, 520-528.
2. Slepian, D.; and Wolf, J. (1973). Noiseless coding of correlated information sources. *IEEE Transactions on Information and Theory*, 19(4), 471-482.
3. Wyner, A.; and Ziv, J. (1976). The rate-distortion function for source coding with side information at the decoder. *IEEE Transactions on Information and Theory*, 22(1), 1-10.
4. Puri, R.; and Ramchandran, K. (2003). PRISM: an uplink-friendly multi-media coding paradigm. 2003 *IEEE International Conference on Acoustics, Speech, and Signal Processing (ICASSP '03)*, 4, IV-856-9.
5. Brites, C.I.C. (2005). *Advances on distributed video coding*. In Instituto Superior Técnico, M.Sc. Thesis, Technical University of Lisbon.
6. Aaron, A.; Zhang, R.; and Girod, B. (2002). Wyner-Ziv coding of motion video. *The Thirty-Sixth Asilomar Conference on Signals, Systems and Computers*, 1, 240-244.
7. Aaron, A.; and Girod, B. (2002). Compression with side information using turbo codes. *IEEE Conference on Data Compression*, 252-261.
8. Puri, R.; and Ranichandran, K. (2003). PRISM: A "reversed" multimedia coding paradigm. *International Conference on Image Processing*, 1, I-617-20.
9. Fowler, J.E. (2005). An implementation of PRISM using QccPack. *Technical Report MSSU-COE-ERC-05-01*, Mississippi State University.
10. Westerlakena, R.P.; Gunnewiekb, R.K.; and Lagendijk, R.L. (2005). The role of the virtual channel in distributed source coding of video. *IEEE International Conference on Image Processing*, 1, I-581-4.
11. Majumdar, A.; Chou, J.; and Ramchandran, K. (2003). Robust distributed video compression based on multilevel coset codes. *The Thirty-Seventh Asilomar Conference on Signals, Systems and Computers*, 1, 845-849.
12. Qing, L.B.; He, X.H.; and Rui, L. (2007). Modeling non-stationary correlation noise statistics for Wyner-Ziv video coding. *International Conference on Wavelet Analysis and Pattern Recognition*, *ICWAPR* '07, 1, 316-320.
13. Trapanese, A.; Tagliasacchi, M.; Tubaro, S.; Ascenso, J.; Brites, C.; and Pereira, F. (2005). Improved correlation noise statistics modelling frame-based pixel domian Wyner-Ziv video coding. *International. Workshop on Very Low Bitrate Video Coding*, Sardinia, Italy.
14. Du, B.; and Shen, H. (2010). A novel reconstruction approach for pixel-domain distributed video coding. *International Conference on Future Computer and Communication* (*ICFCC*), 2, V2-614-V2-618.
15. Slowack, J.; Mys, S.; Skorupa, J.; Lambert, P.; Van de Walle, R.; and Grecos, C. (2009). Accounting for quantization noise in online correlation noise estimation for distributed video coding. *Picture Coding Symposium*, *PCS 2009*, 1-4.
16. Westerlaken, R.P.; Borchert, S.; Gunnewiek, R.K.; and Lagendijk, R.L. (2006). Dependency channel modeling for a LDPC-based Wyner-Ziv video compression scheme. *2006 IEEE International Conference on Image Processing*, 277-280.

17. Brites, C.; and Pereira, F. (2008). Correlation noise modeling for efficient pixel and transform domain Wyner-Ziv video coding. *IEEE transactions on Circuit and Systems for Video Technology*, 18(9), 1177-1190.
18. Li, Y.; Ma, S.; Zhao, D.; and Gao, W. (2009). Modeling correlation noise statistics at decoder for multi-view distributed video coding. *IEEE International Symposium on Circuits and Systems*, *ISCAS*, 2597-2600.
19. Stankovic,V.; Liveris, A.D.; Xiong, Z.; and Georghiades, C.N. (2004). Design of Slepian-Wolf codes by channel code partitioning. *IEEE Proceedings of Data Compression Conference*, 4, 302-311.
20. Xiong, Z.; Liveris, A.D.; and Cheng, S. (2004). Distributed source coding for sensor networks. *IEEE Signal Processing Magazine*, 21(5), 80-94.
21. Pradhan, S.S.; and Ramchandran, K. (2003). Distributed source coding using syndromes (DISCUS): Design and construction. *IEEE Transactions on Information Theory*, 4993), 626-643.
22. Brites, C.; Ascenso, J.; Pedro, J.Q.; and Pereira, F. (2008). Evaluating a feedback channel based transform domain Wyner-Ziv video codec. *Signal Processing: Image Communication*, 23(4), 269-297.
23. Chien, W.J.; Karam, L.J. and Abousleman, G.P. (2008). Rate-distortion based selective decoding for pixel-domain distributed video coding. *15th International Confeence on Image Procesing, ICIP 2008*, 1132-1135.
24. Prakash, I.; Prabhakaran, V.M.; and Kannan, R. (2003). Towards a theory for video coding using distributed compression principles. *2003 International Conference on Image Processing*, *ICIP 2003*, 2, II-687-90.
25. Meyer, P.F.A.; Westerlaken, R.P.; Gunnewiek, R.K.; and Lagendijk, R.L. (2005). Distributed source coding of video with non-stationary side-information. *Proceedings of Conference on Visual Communications and Image Processing*, 857-866.
26. Yovanof, G.S.; and Liu, S. (1996). Statistical analysis of the DCT coefficients and their quantization error. *1996 Conference Record of the Thirtieth Asilomar Conference on Signals, Systems and Computers*, 1, 601-605.